

Development of net-shape cast aluminium–yttrium alloy wires and their solidification structures

H. SODA, A. McLEAN, J. SHEN

Department of Metallurgy and Materials Science, University of Toronto, Toronto, Ontario, Canada

Q. XIA*

Department of Metallurgy, Wuhan Iron and Steel University, Wuhan, People's Republic of China

G. MOTOYASU*

Department of Metallurgical Engineering, Chiba Institute of Technology, Chiba-ken, Japan

M. KOROTKIN, K. YAN

Cametoid Advanced Technologies Inc., Whitby, Ontario, Canada

Cast-aluminium–1.5–7 wt % yttrium alloy wires were produced by the heated mould (Ohno Continuous Casting) process with a typical casting speed of 1.1 m min^{-1} . Using a 2 mm diameter channel bore and positioning the solidification front outside the mould, it was possible to cast wires of 1.6–1.9 mm diameter with uniform chemical composition along the length of the wire. Cast wires contained directionally solidified cells or dendrites of α -aluminium with metastable Al_4Y and $\beta\text{-Al}_3\text{Y}$ phases in intercellular or interdendritic regions. At higher casting speeds ($> 1.1 \text{ m min}^{-1}$), the predominant metastable phase was found to be Al_4Y .

1. Introduction

The Ohno Continuous Casting (OCC) process uses a mould heated to a temperature just above the liquidus of the alloy to be cast, with heat being extracted from the molten alloy by means of a cooling device located near the mould. Because the mould is heated, the heat flow is parallel to the casting direction, and unidirectional solidification occurs. Also no crystals nucleate on the mould surface due to the external heat applied to the mould. By contrast, in conventional systems the mould is water-cooled; thus crystals nucleate on the mould surface. This mode of solidification causes friction between the mould and cast strand surfaces. However, friction is reduced or eliminated in the OCC process, permitting the casting of small net-shaped cast products without breakage. Thus, an application of this technology to cast aluminium alloy wires in the range of 1–2 mm diameter, is feasible. It offers the possibility of incorporating optical fibre sensors, ceramic particles and a different metal core into aluminium alloy wires [1–3]. Materials with workability problems can also be cast into the form of wires and rods [4]. Also, the small size of the OCC equipment compared to the conventional water-cooled mould continuous casting systems [5], will allow the production of a small quantity of value-

added aluminium alloy wires for specific purposes. In the present work, an experimental investigation was conducted with the aim of casting aluminium 1.5–7 wt % yttrium alloy wires of 1.6–1.9 mm diameter for the purpose of vacuum-coating applications.

Aluminium-based alloys containing rare-earth elements such as yttrium have been the subject of several studies to develop new materials using rapid solidification [6, 7]. In these studies, melt-spun ribbon strips, 20–70 μm thick, were examined, and the formation of non-crystalline solids and non-equilibrium phases were reported. The cooling rates for a melt-spinning technique are about $10^5\text{--}10^6 \text{ }^\circ\text{C s}^{-1}$ for a ribbon thickness of 20–70 μm [8]. The OCC process can attain or surpass the cooling range of near-rapid solidification ($1\text{--}10^3 \text{ }^\circ\text{C s}^{-1}$) for the casting of aluminium alloy wires of 1.6–1.9 mm diameter [2]. Microstructures of Al–Y alloy produced in the cooling range of the OCC process have not yet been reported, so this aspect was also examined in the present study.

2. Experimental procedure

Fig. 1 shows a schematic illustration of the OCC equipment which consists of a melting furnace, a cylindrical hollow displacer block made of alumina for

*Visiting scientists, University of Toronto.

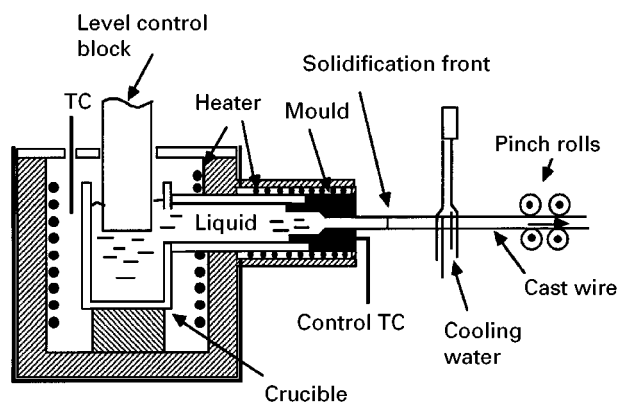


Figure 1 Schematic diagram of the horizontal OCC equipment. TC, thermocouple.

molten metal level control, a graphite mould 105 mm long and 20 mm outside diameter, a cooling device, and pinch rolls for withdrawal of the cast product. The mould has a cylindrical channel, 13 mm long and 2 mm diameter, which determines the maximum diameter of the cast wires. The remainder of the mould cavity was widened to 10 mm diameter in order to assist metal flow. The control thermocouple was positioned approximately 7 mm into the exit side of the mould. The processing parameters are mould temperature, mould-cooler distance, and casting speed. The mould temperature was preset throughout the casting operations at $680 \pm 2^\circ\text{C}$, which is 20°C above the melting temperature of aluminium. Based on differential thermal analysis performed on an Al–Y alloy melt in a graphite crucible, Li *et al.* [9] reported that no reaction took place between the Al–Y melt and the graphite crucible for temperatures below 1377°C . Thus it is reasonable to use graphite as a mould material. Cooling of the wire was obtained using a column of free-falling water from a small tube placed about 30 mm above the cast strand. The amount of cooling water used was $220\text{--}240\text{ mL min}^{-1}$. The mould-cooler distance was adjusted to between 10 and 15 mm. To start casting, a stainless steel tube, 2 mm diameter, was positioned at the mould exit and a small dummy wire was inserted into it. When the temperature attained the set value of 680°C , the molten metal was fed into the mould by lowering the displacer block into the crucible and bringing the metal level to about 20–30 mm above the metal intake connected to the mould. As soon as the molten metal filled the mould, the water was turned on and casting was initiated by moving the pinch rolls. The casting speeds employed were between 0.07 and 1.7 m min^{-1} . The melt stock was prepared by alloying 99.9% aluminium and Al–87% Y master alloy using a vacuum induction furnace.

3. Results and discussion

3.1. Dimensional stability of the cast wire

Figs 2 and 3 show a typical example of the cast aluminium–yttrium alloy wires produced using a casting speed of 1.1 m min^{-1} . The wire exhibited a bright and metallic surface. This indicates that the wire solidified outside the mould [10]. Close observations

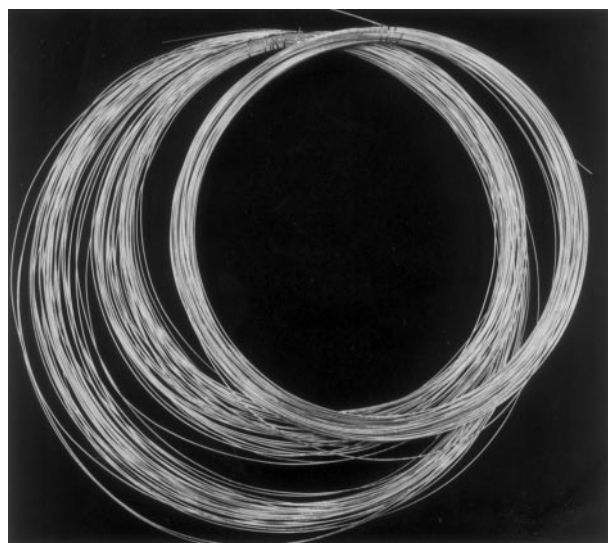


Figure 2 Al–3.1%Y alloy wires of approximately 170 m total length produced with a casting speed of 1.1 m min^{-1} .

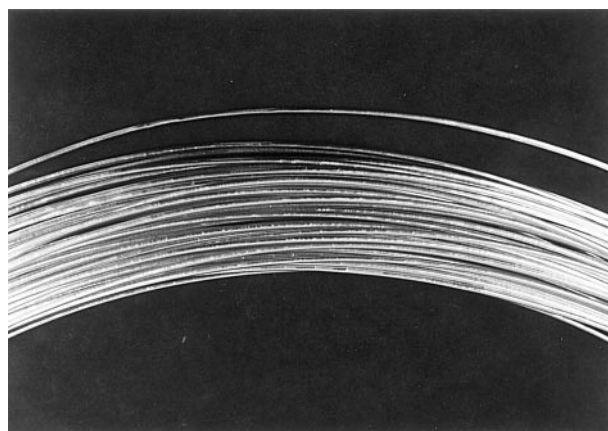


Figure 3 Higher magnification view of the cast wire in Fig. 2.

during casting revealed that the solidification front was, in fact, located outside the mould with the casting speeds ($0.07\text{--}1.7\text{ m min}^{-1}$) used in the present experiment. In most cases, the casting speed was adjusted to 1.1 m min^{-1} at a mould temperature (temperature at the control thermocouple) of 680°C and a mould-cooler distance of approximately 12 mm. Using these casting settings, the solidification front was located approximately 7 mm away from the mould. This speed was the most suitable, although it was possible to cast up to 1.5 m min^{-1} with this particular arrangement. Breakout occurred when the casting speed reached approximately 1.7 m min^{-1} owing to insufficient heat extraction. Because aluminium and yttrium are reactive, the formation of oxide film was observed on the surface of the liquid column, forming an oxide pipe through which the liquid metal continuously flowed. Analysis by Auger electron spectroscopy indicated that the thickness of the oxide film was approximately 20 nm. The oxide pipe was approximately 7 mm long and remained stationary at the mould exit. Thus, it is reasonable to assume that the solidification front existed close to the outer end of the oxide pipe. Fig. 4 shows an example of oxide pipe which was detached from the mould and was carried away with the strand.

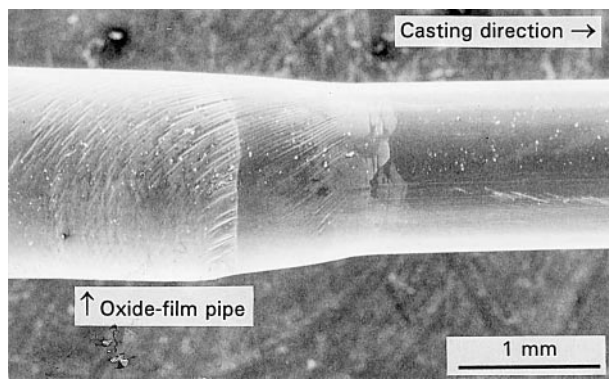


Figure 4 Oxide-film pipe originally formed at the mould exit.

Because the cast strand solidifies between the mould and cooling water location (Fig. 1), the diameter of the wire is directly influenced by the volume of the molten metal that comes out of the mould and the casting speed. With a mould channel of 2 mm diameter, it was possible to produce wires having diameters between 1.6 and 1.9 mm by adjusting the metal head for a given casting speed. Improper metal head adjustment caused either necked-down regions in the wires or a gradual change in diameter. The formation of oxide film on the liquid metal strand also influenced the dimensional stability of the cast wire. With the formation of a thick oxide pipe, the diameter tended to be smaller due to the throttling effect created by the oxide pipe, and detachment of this pipe from the mould caused a shift in diameter. The dimensional stability of the wire is also strongly affected by various mechanical movements transmitted to the solidifying wires. Lateral movements of the cast strand caused by the pinch rolls produced kinked and wavy wires. The effects of these mechanical movements were significantly alleviated by simply placing a 3 mm inner diameter tubular support made of alumina just behind the water-cooling location. Fig. 5a shows variations in the diameter along the 150 m length of cast wire, the diameter of which was measured every 1.18 m. The wire diameter ranged between 1.4 and 1.85 mm, averaging 1.7 mm with a standard deviation of 0.09 mm. Several large diameter drops were due to insufficient metal head; this can be improved with tighter control of the metal head level. For example, when better attention was paid to the metal level in the crucible by pushing the level control device continuously downward in accordance with the casting speed, in order to keep the metal head at a constant level, the wire diameter, measured every 1.16 m, was maintained at 1.72 mm with a standard deviation of 0.04 mm, as shown in Fig. 5b. This may be further improved by controlling the formation of oxide pipe at the mould exit, i.e. avoiding accumulation of the oxide matter at the mould exit. To achieve this, the solid-liquid interface may be located right at the mould exit by reducing the mould temperature and mould-cooler distance.

3.2. Microstructure

Fig. 6 shows backscattered scanning electron micrographs of Al-1.5%Y and 3.6%Y alloy ingots cast into

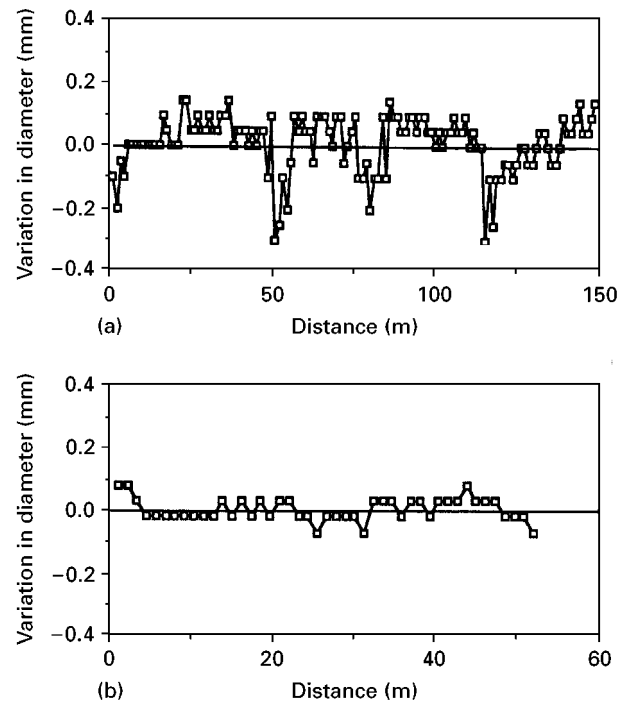


Figure 5 Variation in diameter along the length of the cast wire. (a) Using intermittent metal level control, the average wire diameter is 1.7 mm with a standard deviation of 0.09 mm. (b) Using continuous level control, the average diameter is 1.72 mm with a standard deviation of 0.04 mm.

a cast-iron mould of ~ 10 cm diameter. The 1.5%Y alloy ingot contains large primary aluminium phases and eutectic zones with a rod-type structure, whereas the interdendritic morphology of the 3.6%Y alloy ingot was mainly of the lamellar type. The 7%Y alloy ingot (not shown) exhibited a similar structure to that of the 3.6%Y ingot. Fig. 7 shows typical scanning electron micrographs of an OCC wire containing 3.6%Y produced with a casting speed of 0.2 m min^{-1} . The fine and uniform cast structure was observed throughout the cross-section of the wire. As expected from the casting configuration of the OCC system, the longitudinal section of the wire exhibited a unidirectional structure in the casting direction (Fig. 7b). The transverse section exhibited an irregular cellular structure of α -aluminium with an intercellular region containing yttrium. At a magnification of $\times 2000$, it was not possible to resolve this intercellular region for the 3.6%Y alloy wire, although for the Al-7%Y alloy wire produced with a low casting speed of 0.2 m min^{-1} , a duplex interdendritic region was observed at the same magnification. Yttrium concentration in the intercellular region was confirmed by energy dispersive X-ray (EDX) analysis (Fig. 8). Based on the appearance of the yttrium concentration in the form of separate distinct spots, this intercellular region may also be duplex eutectic.

The formation of metastable phases is known to occur in rapidly cooled aluminium-based alloys. In the aluminium-yttrium system, the occurrence of β - Al_3Y , Al_4Y or $\text{Al}_4\text{Y}/\text{Al}_{11}\text{Y}_3$ has been reported [7, 9]. For example, Li *et al.* [9] reported that melt-spun ribbons of the Al-26.8 wt% (10 at %) Y alloy, prepared below the critical wheel speeds (e.g. 40 m s^{-1} at an ejecting temperature of 1077°C), contained a

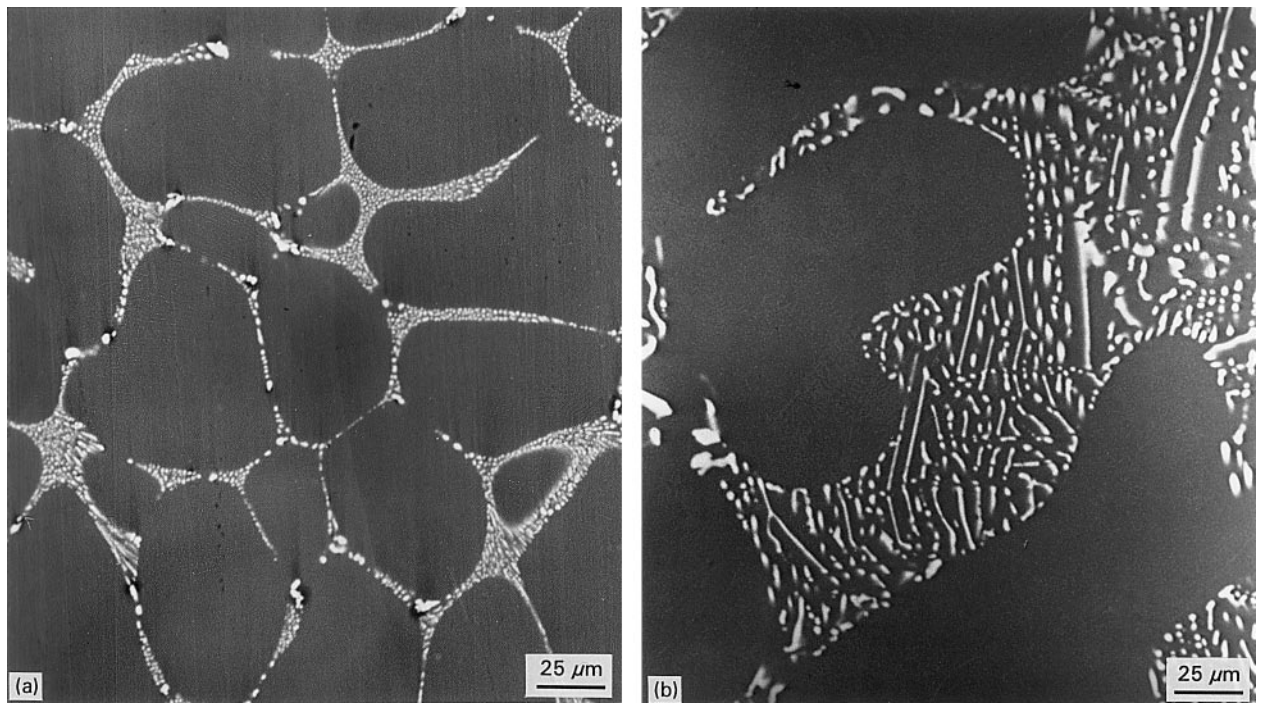


Figure 6 Backscattered scanning electron micrographs of (a) Al-1.5%Y and (b) 3.6%Y alloy ingots used as melt stock, showing massive primary aluminium phases with eutectic zones.

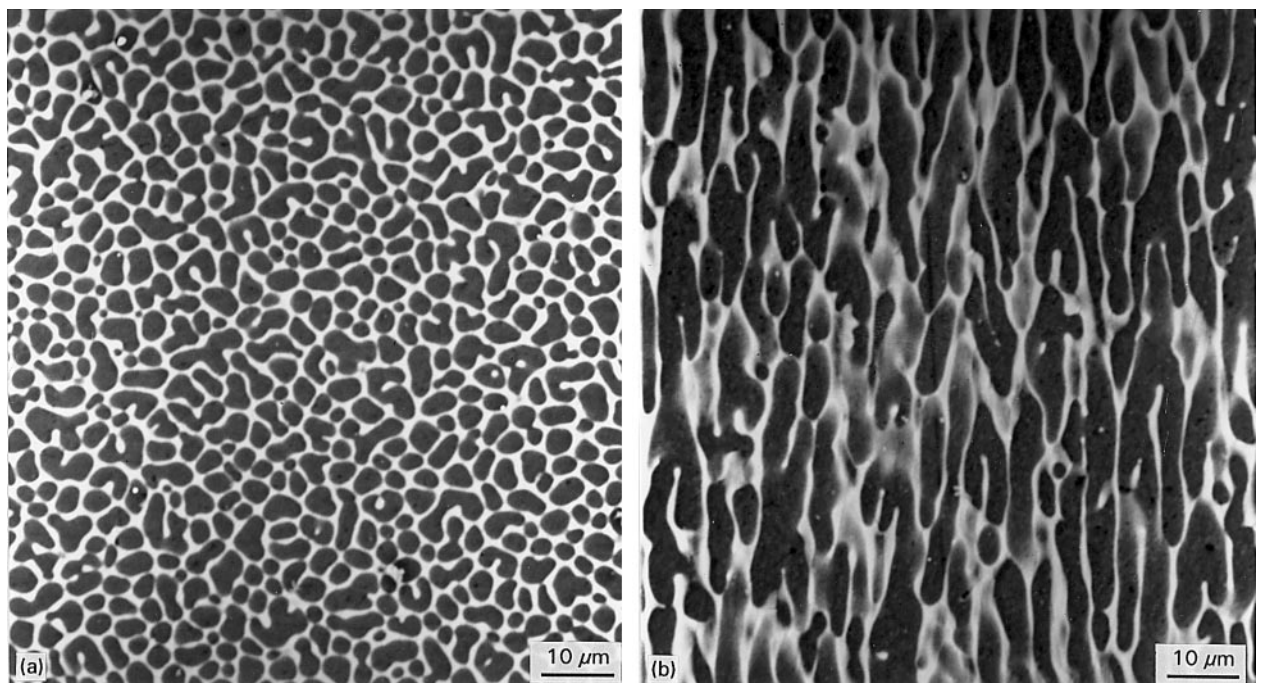


Figure 7 Backscattered scanning electron micrograph of cast Al-3.6%Y alloy wire. Casting speed was 0.2 m min^{-1} . The dark area is aluminium and the white area contains aluminium-yttrium compounds: (a) transverse, and (b) longitudinal sections.

mixture of the amorphous phase and metastable β - Al_3Y and Al_4Y . Also, Li *et al.* [11] noted that the crystallization of Al_4Y phase occurred during the annealing of melt-spun amorphous ribbons, and Al_4Y transformed into β - Al_3Y and further into equilibrium α - Al_3Y with a higher annealing temperature and an extended time [11].

In the present investigation, X-ray diffraction (XRD) analysis was performed using CuK_α radiation with step-scans of 0.01° and a scan speed of 4° min^{-1} on some of the original ingots and OCC wires. Fig. 9

shows the results of XRD examinations on the Al-7%Y alloy samples. In accordance with the equilibrium phase diagram, α -aluminium and α - Al_3Y phases are expected. However, the XRD spectrum showed that the cast ingot contained only α -aluminium and metastable β - Al_3Y . Most of the diffraction peaks from the aluminium-yttrium compounds present in the OCC wires differed from those of the ingot, indicating that these compounds have different compositional stoichiometry from Al_3Y . It was found that OCC wires, in addition to α -aluminium and β - Al_3Y

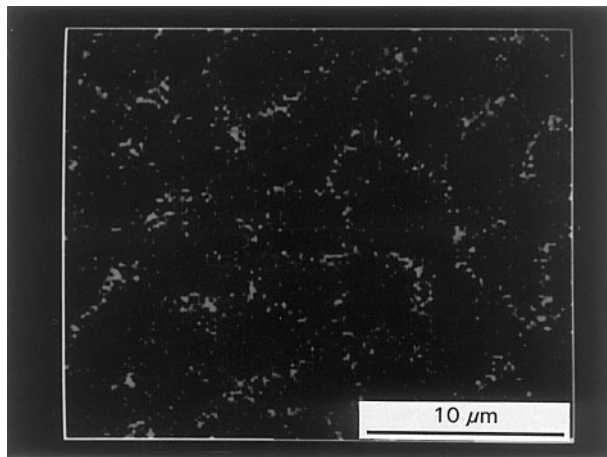


Figure 8 X-ray mapping showing yttrium concentration in the intercellular region of the cast wire containing 3.6% Y.

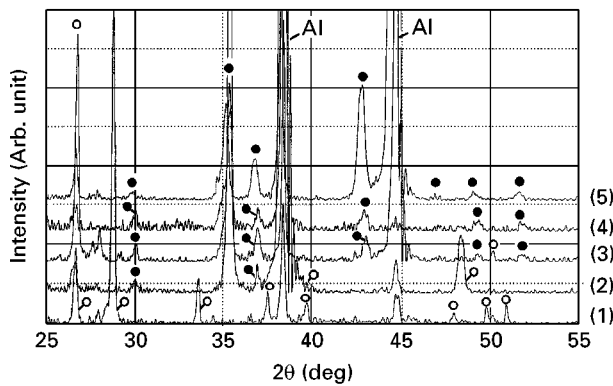


Figure 9 XRD spectra from (1) Al-7%Y ingot and (2-5) cast 7%Y wires produced with various casting speeds: (2) 0.2, (3) 0.6, (4) 1.1, and (5) 1.3 m min⁻¹. (●) Al₄Y, and (○) β-Al₃Y.

phases, contained a metastable phase, the diffraction spectra of which was identified as Al₄Y [7, 11]. It is clear that with faster casting speeds of 1.1 and 1.3 m min⁻¹, the aluminium–yttrium compounds were mostly Al₄Y. This Al₄Y phase was also found to exist in the wire produced with a casting speed as low as 0.2 m min⁻¹. After annealing at 500 °C for 3 h, the diffraction spectrum from the cast wire became identical to that from the ingot, which exhibited the presence of only α-aluminium and β-Al₃Y (Fig. 10). These results also reconfirmed the formation of a metastable Al₄Y phase in the as-cast OCC wires. The XRD results from the Al-1.5% Y alloy wires showed similar spectra to that observed in the Al-7%Y alloy wires with change in casting speed. However, the wire produced with a casting speed of 0.07 m min⁻¹ contained only α-Aluminium and β-Al₃Y phases equivalent to those found in the cast ingot.

The cooling rates can be estimated roughly from cell and dendrite arm spacing. Spacings were measured by employing a line intersect method from micrographs and plotted as a function of casting speed in Fig. 11. For casting speeds between 0.07 and 1.4 m min⁻¹, spacings ranged between 11 and 1.6 μm, respectively, which can be related to the cooling rates reported in references or using the relation $D = 50A^{-0.33}$, where D is the secondary arm spacing or

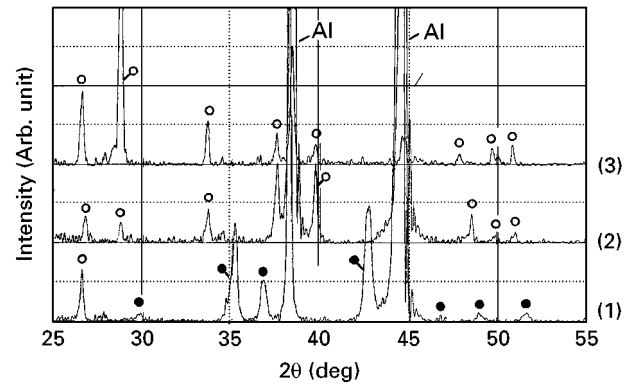


Figure 10 XRD spectra from Al-7%Y wires cast at 1.3 m min⁻¹ (1) before and (2) after annealing, and (3) spectrum from the ingot. (●) Al₄Y and (○) β-Al₃Y.

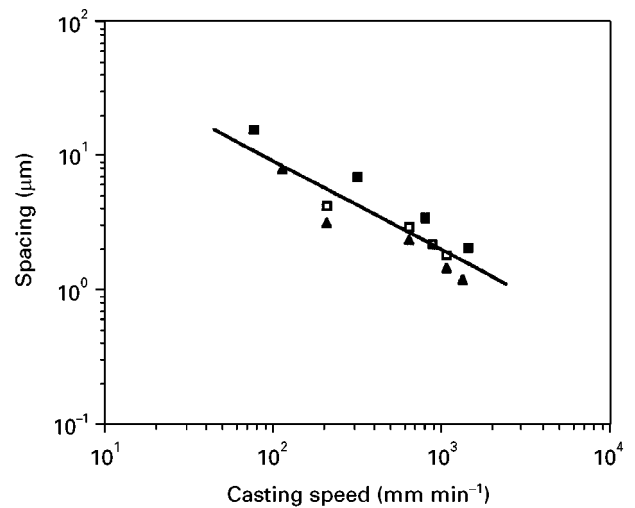


Figure 11 Cell and secondary dendrite arm spacing versus casting speed. (■) 1.5%Y, (□) 3.6%Y, (▲) 7.0%Y.

cell spacing (μm) and A is the cooling rate (°C s⁻¹) [12–15]. The estimated cooling rates were found to be in the range 10²–10⁴ °C s⁻¹. Thus, it can be concluded that an Al₄Y phase exists only in the cast wires which solidify with cooling rates greater than approximately 10² °C s⁻¹.

The solidification morphology is known to change from cellular to dendritic form with an increase in solidification rate for a given temperature gradient. It was found that for the Al-3.6%Y alloy wires the microstructure changed from cellular (Fig. 7) to dendritic structure (Fig. 12) at high casting speeds of 1.1 and 1.3 m min⁻¹, while the Al-7%Y alloy wires exhibited dendritic morphology even at the slow casting speed of 0.2 m min⁻¹ (Fig. 13). Fig. 14 shows a regime of cellular and dendritic morphology in relation to casting speed and composition.

3.3. Compositional variation

It is essential for cast wires to have macroscopically uniform chemical composition along the length of the wire. Cast wires were analysed for yttrium using the neutron activation technique. The results are plotted in Fig. 15 in terms of deviations from the average yttrium concentration of the wire versus points of

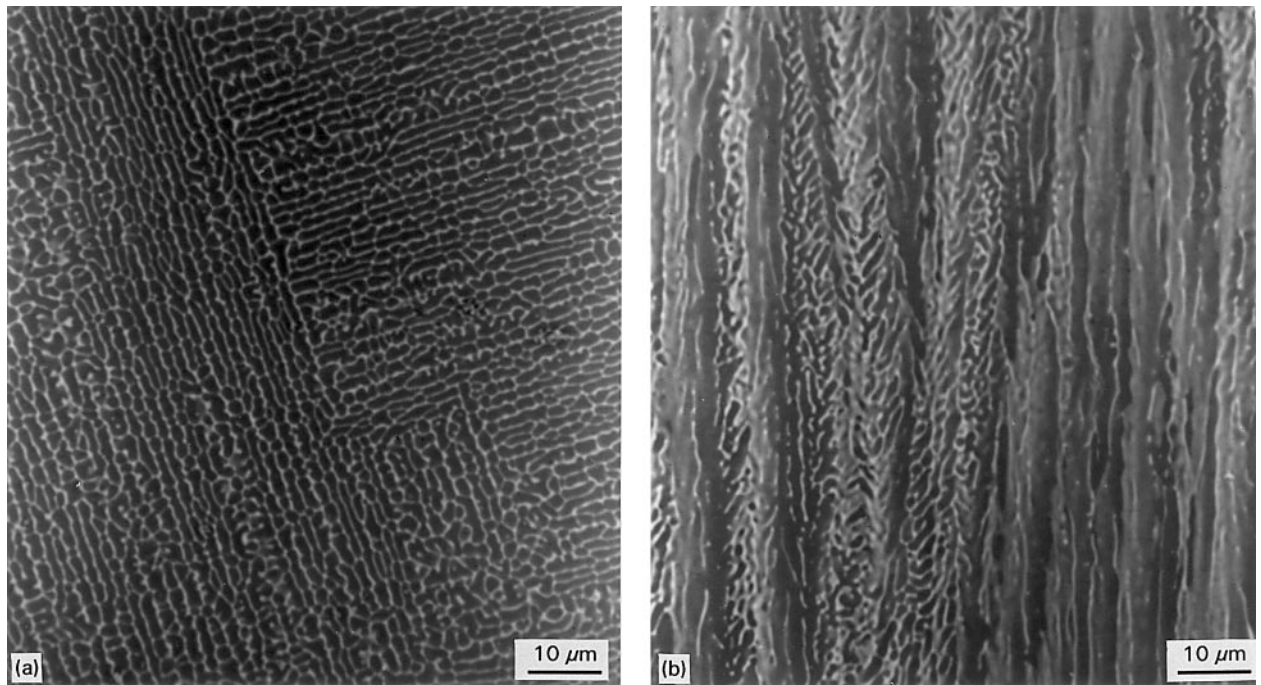


Figure 12 Backscattered scanning electron micrograph of cast Al-3.6%Y wire, produced with a casting speed of 1.3 m min^{-1} , showing dendrite structure: (a) transverse and (b) longitudinal section.



Figure 13 Backscattered scanning electron image (longitudinal section) of Al-7%Y alloy wire showing dendrite structure. Casting speed was 0.2 m min^{-1} .

analysis along the length of the wire. The composition was found to remain essentially constant.

4. Conclusions

An experimental study was conducted with the aim of continuously casting Al-1.5-7 wt %Y alloy wires, of 1.6-1.9 mm diameter. The following results were found.

1. With the use of a 2 mm diameter channel bore and by adjusting the metal head level, wires of 1.7 mm

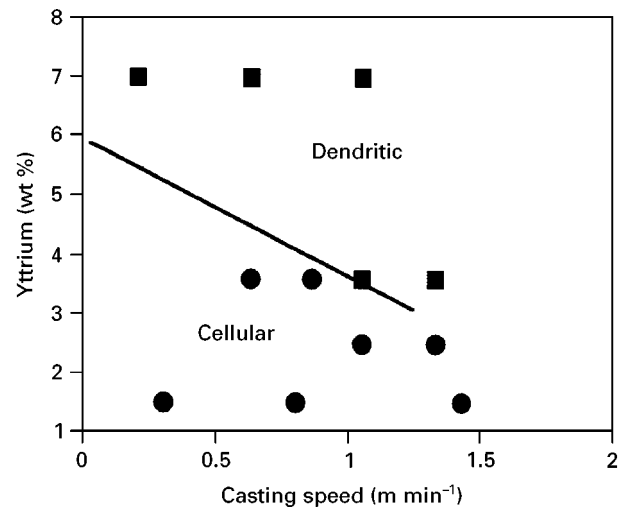


Figure 14 Relationship between casting speed, initial solute concentration and solidification morphology.

diameter with a standard deviation of 0.09 mm could be cast at a typical casting speed of 1.1 m min^{-1} .

2. To achieve better dimensional stability, tighter control of metal head must be maintained and the solid-liquid interface should be brought to the mould exit in order to avoid the formation of an oxide film.

3. Wires with fine, unidirectionally solidified cellular or dendritic microstructures could be cast with cell or dendrite arm spacing ranging between 1.6 and 11 μm

4. Chemical composition remained constant along the length of the wires.

5. Cast wires, produced with casting speeds $> 0.2 \text{ m min}^{-1}$, contained α -aluminium metastable Al_4Y , and β - Al_3Y phases. With higher casting speeds (1.1 and 1.3 m min^{-1}), the Al-Y phase mainly existed as Al_4Y . At the lowest casting speed employed

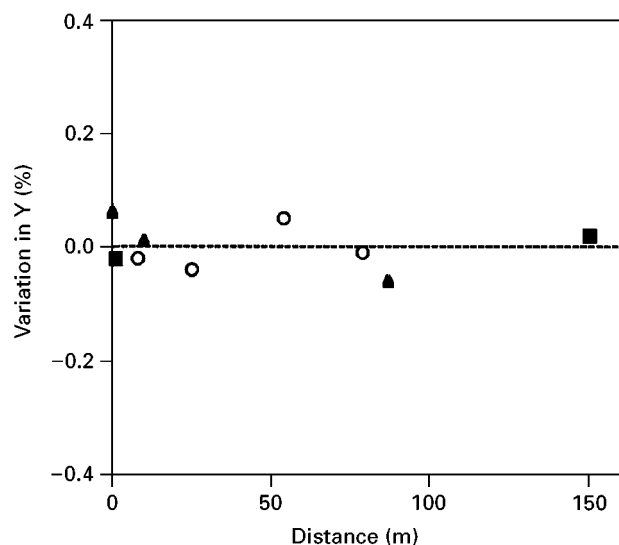


Figure 15 Variation in yttrium concentration along the length of the cast wire. Casting speed was between 1 and 1.3 m min^{-1} . (■) Al-1.9%Y, (▲) Al-2.5%Y, (○) Al-3.6%Y.

(0.07 m min^{-1}), the wires do not contain the Al_4Y phase but only α -aluminium and β - Al_3Y phases.

6. The corresponding cooling rates estimated from cell and dendrite arm spacing for casting speeds between 0.07 and 1.4 m min^{-1} were in the range 10^2 – $10^4 \text{ }^\circ\text{C s}^{-1}$.

7. The Al_4Y phase existed in cast wires which solidified with cooling rates greater than $10^2 \text{ }^\circ\text{C s}^{-1}$.

Acknowledgements

Financial support from the Manufacturing Research Corporation of Ontario (MRCO) and the Ontario Centre for Materials Research (OCMR) is gratefully acknowledged.

References

1. H. SODA, G. MOTOYASU, A. MCLEAN, C. K. JEN and O. LISBOA, *J. Mater. Sci. Technol.* **11** (1995) 1169.
2. A. McLEAN, H. SODA, Q. XIA, A. K. PRAMANICK, A. OHNO, G. MOTOYASU, T. SHIMIZU, S. A. GEDEON and T. NORTH, *Compos. Part A*, in press.
3. H. SODA, A. ICHINOSE, G. MOTOYASU, A. OHNO and A. McLEAN, *Cast Metals* **5** (2) (1992) 95.
4. T. SHIMIZU, H. YAMAZAKI, H. SODA and A. McLEAN, in "Proceedings of 32nd Annual Conference of Metallurgists on Developments and Applications of Ceramics and New Metal Alloys", edited by R. A. L. Drew and H. Hostaghaci (Metallurgical Society of CIM, Montreal, Canada, 1993) p. 541.
5. D. A. GRANGER, L. D. HAMMAR and E. SALAS, *Wire J. Int.* **27** (2) (1994) 88.
6. A. INOUE, K. OHTERA and T. MASUMOTO, *Jpn J. Appl. Phys.* **27** (1988) L736.
7. B. DILL, Y. LI, M. AL-KHAFAJI, W. M. RAINFORTH, R. A. BUCKLEY and H. JONES, *J. Mater. Sci.* **29** (1994) 3913.
8. B. CANTOR, in "Science and Technology of the Undercooled Melt – Rapid Solidification Technologies" edited by P.R. Sahm, H. Jones and C.M. Adam, NATO ASI Series E: Applied Science, no. 114 (Martinus Nijhoff, Dordrecht, The Netherlands, 1986) p. 3.
9. Q. LI, E. JOHNSON, A. JOHNASSEN and L. SARHOLT-KRISTENSEN, *J. Mater. Res.* **7** (1992) 2756.
10. H. SODA, G. MOTOYASU, F. CHABCHOUB, H. HU and A. McLEAN, *Cast Metals* **6** (4) (1994) 225.
11. Q. LI, E. JOHNSON, M. B. MADSEN, A. JOHANSEN and L. SARHOLT-KRISTENSEN, *Philos. Mag. B* **66** (1992) 427.
12. E. J. LAVERNIA, J. D. AYERS and T. S. SRIVATSAN, in "Rapid Solidification Technology", edited by T. S. Srivatsan and T. S. Sudarshan (Technomic Inc., Lancaster, PA, 1993) p. 315.
13. W. G. J. BUNK, *Mater. Sci. Eng. A* **134** (1991) 1087.
14. M. C. FLEMINGS, in "Proceedings of F. Weinberg International Symposium on Solidification Processing", edited by J. E. Lait and I. V. Samarasekera, vol. 20 (Pergamon, New York, 1990) p. 173.
15. H. JONES, *J. Mater. Sci.* **19** (1984) 1043.

Received 3 January
and accepted 18 March 1996